Construction and Building Materials 108 (2016) 139–145

Contents lists available at ScienceDirect

Construction and Building Materials

journal homepage: www.elsevier.com/locate/conbuildmat

Assessing the effect of wood acetylation on mechanical properties and extended creep behavior of wood/recycled-polypropylene composites

Ke-Chang Hung, Tung-Lin Wu, Yong-Long Chen, Jyh-Horng Wu *

Department of Forestry, National Chung Hsing University, Taichung 402, Taiwan

HIGHLIGHTS

- Mechanical and creep properties of WRPCs with acetylated wood particles were studied.
- The TTSP-predicted creep compliance curve fit well with the long-term experimental data.
- The creep resistances of all acetylated WRPCs were improved 11–41% over a 30-year period.
- WRPC with 13% WPG of acetylated wood particles exhibited the best performance.

GRAPHICAL ABSTRACT

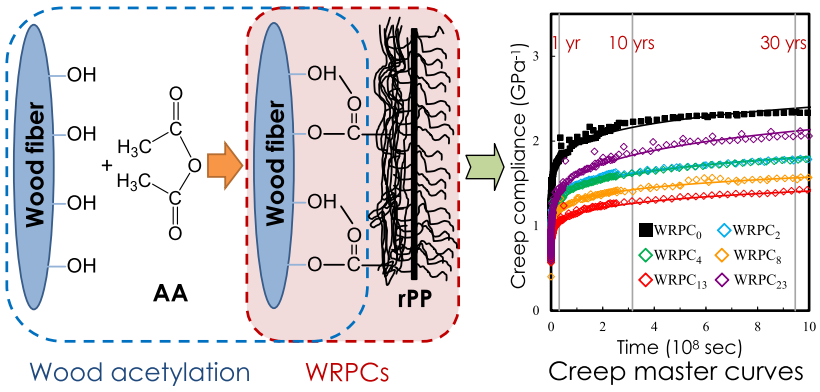

ARTICLE INFO

Article history:
Received 2 October 2015
Received in revised form 20 January 2016
Accepted 24 January 2016
Available online 5 February 2016

Keywords:
Wood/recycled-polypropylene composite
Acetylation
Creep behavior
Mechanical property
Time–temperature superposition principle

ABSTRACT

This study investigates the effect of wood acetylation on the mechanical properties and creep resistance of wood/recycled-polypropylene composites (WRPCs) using the time–temperature superposition principle (TTSP). The results revealed that the flexural and tensile strength of WRPCs increased with increasing weight percent gain (WPG) of acetylated wood particles up to 13%. Additionally, the TTSP-predicted creep compliance curve fit well with the long-term experimental data. The creep resistance of WRPCs with acetylated wood particles was greater than that of WRPCs with unmodified wood particles, especially for the WRPC with 13% WPG of acetylated wood particles.

1. Introduction

Over the past decade, wood–plastic composites (WPCs), in which renewable and low-cost natural fibers are added as reinforcement to the plastic composite, have gained popularity and found important applications in recovery, reuse and recycling of a variety of byproducts from industrial use of natural resources. These WPCs are of great interest in various applications due to such advantages as low-density, low equipment abrasiveness, high stiffness and strength, low maintenance requirements, and biodegradability [1]. However, incompatibility between hydrophilic lignocellulosics and hydrophobic thermoplastics results in poor interfacial interaction. Thus, to overcome this problem, several physical and chemical approaches have been used to modify the lignocellulosic materials by increasing their hydrophobicity [2,3] and improving their dimensional and thermal stabilities [4,5].

* Corresponding author.
E-mail address: eric@nchu.edu.tw (J.-H. Wu).

http://dx.doi.org/10.1016/j.conbuildmat.2016.01.039
0950-0618/

Among these various approaches, wood acetylation with acetic anhydride has received the most attention.

The conventional acetylation process includes impregnation of dried wood with a liquid-phase acetic anhydride before external heat is applied. However, the downside to this method is that the process is time-consuming and requires large quantities of modification agent. Therefore, the chemical reagent is used in the vapor phase because the reactivity of the reagent in the vapor phase is higher than in the liquid phase. As a result, acetylation with acetic anhydride *via* a vapor phase reaction offers certain benefits, such as reduced reagent consumption, decreased reaction time, and minimized environmental impact [6]. The best-known virgin thermoplastics used as the matrix in WPC products are high and low density polyethylene (HDPE and LDPE) and polypropylene (PP) [7,8]. In addition, it is well known that all of the recycled plastics that can be melted and processed below the degradation temperature of wood or other lignocellulosic fillers are commonly suitable for manufacturing WPCs [9]. Thus, in the past decade, the use of recycled thermoplastics also has been considered for manufacturing of WPCs [10–12]. However, one of the disadvantages of this approach is changes in the WPC mechanical properties with temperature, which leads to limits in wider applications. Therefore, it is also important to investigate the temperature sensitive properties of WPCs, e.g., creep behavior, because WPCs exhibit a strong time–temperature dependent response. Moreover, it is time-consuming and expensive to conduct full-scale creep tests on a normal time scale. In this study, an accelerated creep test based on the time–temperature superposition principle (TTSP) was implemented to predict the long-term creep response. Methods that use this principle have been employed to confirm that TTSP is applicable to various WPCs [13–17].

To date, investigations into WPCs have primarily focused on the effects of various attributes on the thermal and mechanical properties of the composites (e.g., fiber type, fiber loading, functional additives, and fiber modification) to increase the compatibility between the hydrophilic natural fiber and hydrophobic polymeric matrix [3,18–21]. However, little information is available with respect to the effect of wood acetylation on the creep behavior of WPCs. Therefore, in addition to qualification of the physical properties and static mechanical properties of these materials, an objective of the current study was to investigate the time–temperature dependent response and extended creep behavior of WPCs with unmodified and various acetylated wood particles using the TTSP. In addition, different extents of acetylated wood particles were prepared using the vapor phase reaction method in this study.

2. Materials and methods

2.1. Materials

Japanese cedar (*Cryptomeria japonica* D. Don) sapwood was sourced from the experimental forest of the National Taiwan University. Wood particles were prepared by hammer milling and sieving, and particles between 30 and 60 mesh (250–595 μm) were investigated. Recycled-polypropylene (rPP) with a melt index of 3.7 g/10 min and a density of 910 kg/m^3 was purchased from Orbit Polymers Co., Ltd. (Taichung, Taiwan). Acetic anhydride was purchased from the Sigma–Aldrich Chemical Co. (St. Louis, MO, USA). The other chemicals and solvents used in this experiment were of the highest quality available.

2.2. Acetylation

Wood particles were acetylated with acetic anhydride using the vapor-phase reaction method reported in our previous study [6]. Before the reaction, the wood particles were Soxhlet-extracted with acetone for 8 h, and then dried at 105 °C for 12 h. The reaction conditions for different extents of acetylated particles are shown in Table 1. At the end of the reaction, the acetylated wood particles were washed with distilled water and Soxhlet-extracted with acetone for 8 h. Finally, the acetylated wood particles were dried at 105 °C for 12 h. The weight percent gain (WPG) of the wood materials was calculated based on the oven-dried method.

Table 1
Reaction conditions for different extents of acetylated wood particles.

Wood particles	Wood:acetic anhydride (g:mmol)	Reaction time (min)	Particle weight gain (%)
WPG 2	1:2	120	1.6 ± 0.2
WPG 4	1:4	120	4.4 ± 0.8
WPG 8	1:7	120	7.6 ± 0.1
WPG 13	1:20	120	12.7 ± 0.6
WPG 23	1:40	120	23.3 ± 0.3

2.3. Composite panel manufacture

Manufacture of wood/rPP composites (WRPCs): The flat platen pressing process was applied as reported in our previous papers [22,23]. The weight ratio of the oven-dried wood particles (moisture content <3%) to rPP powder was 10:90. The expected density of the WRPCs was 900 kg/m^3. The dimensions of the WRPC samples were 300 mm × 200 mm with a thickness of 4 mm. All of the WRPCs were produced in a two-step pressing process described as follows: (1) hot pressing (2.5 MPa) at 200 °C for 3 min and (2) finishing with cold pressing until the temperature of WRPCs decreased to 30 °C.

2.4. Mechanical properties

Flexural and tensile tests were performed according to the ASTM D790-10 [24] and ASTM D638-14 [25] standards, respectively. A specimen size of 80 mm × 16 mm with a thickness of 4 mm was used to determine modulus of rupture (MOR) and modulus of elasticity (MOE) in a three-point static bending test with a loading speed of 1.7 mm/min and a span of 64 mm. A dumbbell-shaped (Type I) test specimen with a thickness of 4 mm was used for tensile test at a tensile speed of 5 mm/min. Five specimens of each blend were tested at 20 °C. The samples were conditioned at 20 °C and 65% relative humidity (RH) for two weeks before testing.

2.5. Creep test

The short-term accelerated creep tests on the WRPCs were measured in three-point bending mode *via* dynamic mechanical analysis (DMA) (DMA 8000, PerkinElmer) at a frequency of 1 Hz. The dimensions of the sample were 30 mm × 10 mm with a thickness of 4 mm. With a real-time short-term creep response at elevated temperatures, TTSP is used to predict the long-term creep performance of the composites. The creep compliance is given by $S(T_{ref}, t) = S(T_{elev}, t/\alpha_T)$, where S is the creep compliance as a function of temperature and time, T_{ref} is the reference temperature, T_{elev} is the elevated temperature, and α_T is the shift factor. The master curve of creep compliance was determined by DMA. Creep and creep recovery cycles were conducted at isotherms between 20 °C and 70 °C at intervals of 5 °C. A three-point bending mode with a span of 40 mm was used. For each isotherm, 20% of the average flexural strength was applied for 1 h followed by a 1 h recovery period. In addition, long-term creep tests in bending were conducted to serve as a basis of comparison with the results from short-term accelerated creep tests. The tests were conducted under a conditioned environment (20 °C and 65% RH) for 775 days. The dimensions of the sample were 80 mm × 16 mm with a thickness of 4 mm. The applied loading was 20% of the average flexural strength, and the data for creep displacement were recorded by a data logger.

2.6. X-ray diffraction measurement

The X-ray diffractograms were obtained with a MAC science MXP18 analyzer (Japan), and wood samples were prepared by powdering. The diffraction patterns were measured from $2\theta = 2°$ to 35° using CuKα_1 radiation at 40 kV and 30 mA. The crystallinity index (*CrI*) of the wood particle was calculated according to the following equation [26]:

$$CrI(\%) = \frac{I_{002} - I_{am}}{I_{002}} \times 100 \quad (1)$$

where I_{002} is the maximum intensity of the 002 lattice reflection of the cellulose crystallographic form at $2\theta = 22°$, and I_{am} is the intensity of diffraction of the amorphous material at $2\theta = 18°$.

2.7. Scanning electron microscopy

Scanning electron microscopy (SEM) was used to examine the morphology of wood particles and plastics in the composites. After the tensile test, the fracture surfaces of composites were dried and sputtered with gold. A JEOL JSM-6330F SEM (Japan) instrument equipped with a field emission gun and an acceleration voltage of 2.8 kV was used to collect SEM images for the composite specimen. The samples were viewed perpendicular to the fractured surface.

2.8. Statistical analysis

All results are expressed as the mean ± SD. The significance of the difference was calculated using Scheffe's test, with values of $P < 0.05$ considered statistically significant.

3. Results and discussion

3.1. Physical and mechanical properties of WRPCs

The density, moisture content, and static mechanical properties of the WRPCs are summarized in Table 2. In general, density and moisture content might directly affect the flexural properties of a polymer composite. No significant difference in density was noted among all of the composites (~900 kg/m^3). However, lower moisture content that was found in the $WRPC_{13}$ and $WRPC_{23}$, and both composites were significantly different from the $WRPC_0$. This phenomenon could be influenced by substitution of the amount of hydroxyl groups by acetyl moieties after acetylation when the WPG of acetylated wood particles reached 13%, leading to the reduction of hydrophilicity of wood particles.

Table 2 shows that the MOR decreased from 51 MPa to 43 MPa when 10 wt% of unmodified wood particles was added into an rPP matrix. This phenomenon may be attributed to the wide polarity differences of the surfaces that retard the interaction of polymer/-wood particle bonding [17,27]. However, the MOR of WRPCs with acetylated wood particles is greater than that of $WRPC_0$, especially for the $WRPC_8$ and $WRPC_{13}$, whose values were similar to that of neat rPP. When the WPG of acetylated wood particles reached 2%, 4%, 8%, and 13%, the MOR values of those WRPCs were 46 MPa, 46 MPa, 48 MPa, and 50 MPa, respectively. The acetylation of wood particles improved the MOR of WPC, resulting from the improved interfacial interaction between the wood particle and polymer [28]. In contrast, the MOR of $WRPC_{23}$ was similar to $WRPC_0$. For the MOE, the modulus increased with the addition of 10 wt% unmodified wood particles into an rPP matrix, and the MOE increased from 1.8 GPa to 2.1 GPa. Stiffer wood particles play a role in stress transition in a composite, leading to improvement of the flexural properties. A similar effect has also been reported by many researchers [17,29]. In addition, similar to the findings in MOR, the $WRPC_{13}$ exhibited the highest MOE (2.3 GPa) among all WRPCs, and a drastic decrease in the MOE was observed when the WPG of acetylated wood particles exceeded 13%. Similar results were reported by Hung and Wu [3] and Pasquini et al. [30].

Fig. 1 shows the evolution of the X-ray diffraction patterns of acetylated wood particles. The results reveal two diffraction rays for $2\theta = 22°$ and 15° before treatment, and the calculated *CrI* is 38.4%. After acetylation, the former ray due to the 002 plane of crystal lattice was shifted to the amorphous condition of 18–20°, and the other ray corresponding to the reflection of planes 101 and $10\bar{1}$ of the native cellulose lattice gradually vanished

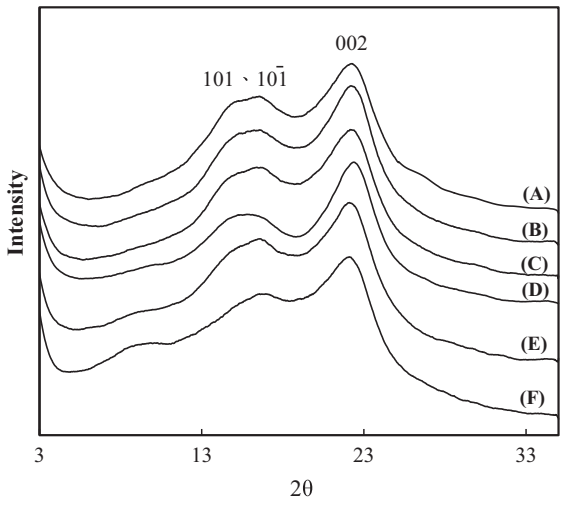

Fig. 1. X-ray diffraction diagrams of different extents of acetylated wood particles. (A) Unmodified; (B) WPG 2; (C) WPG 4; (D) WPG 8; (E) WPG 13; (F) WPG 23.

(Fig. 1B–F). These results are similar to the diagram obtained by Hung and Wu [3] and Thiebaud et al. [31]. In addition, the extent of decrystallization is a function of ester content (or WPG). In other words, the extent of acetylation greatly influenced crystallinity, and thus, a higher extent of acetylation produced a lower *CrI*. However, for all WPG with less than 13% of acetylated wood particles, the *CrI* values ranged from 37.1% to 39.9%, and no significant differences were noted among them. Once the WPG of acetylated wood particles reached 23%, the *CrI* decreased dramatically to 32%. This reduction is nearly congruent with the MOE changes in Table 2. Therefore, it is evident that the MOE of WRPCs is greatly influenced by the crystallinity of lignocelluloses.

Indeed, the tensile property is the best single measure of the quality of lignocellulosic composites because it exhibits sensitivity to the interfacial adhesion between the lignocellulose and the polymer matrix. Table 2 shows that for the tensile modulus, there was no significant difference between neat rPP and $WRPC_0$, but the WRPC with 13% WPG of acetylated wood particles exhibited the highest tensile modulus (2.13 GPa). Furthermore, the tensile strength decreased from 34.4 MPa to 22.3 MPa with the addition of 10 wt% unmodified wood particles into an rPP matrix. The decreased strength could be attributed to the incompatibility between the hydrophilic wood particles and the hydrophobic rPP, which promotes microcrack formation at the interface. The tensile strength of $WRPC_2$ was similar to the $WRPC_0$, but the strength of $WRPC_4$ increased significantly to 25.6 MPa. These results indicate that when the WPG of acetylated wood particles was only 4%, the particles provide sufficient interfacial adhesion with the plastic matrix, leading to a more efficient transfer of stress along the wood

Table 2
Effects of wood acetylation on physical and mechanical properties of WRPCs.

Specimen	Wood/rPP (wt%)	WPG of acetylated wood (%)	Air-dried density (kg/m^3)	Moisture content (%)	Flexural properties		Tensile properties		
					MOE (GPa)	MOR (MPa)	Modulus (GPa)	Strength (MPa)	Elongation at break (%)
Neat rPP	0/100	–	897 ± 9^a	–	1.80 ± 0.06^c	51.6 ± 1.0^a	1.90 ± 0.04^c	34.4 ± 0.4^a	7.1 ± 0.9^a
$WRPC_0$	10/90	0	890 ± 19^a	0.32 ± 0.04^a	2.10 ± 0.18^b	43.4 ± 2.1^{cd}	1.95 ± 0.16^{bc}	22.3 ± 1.6^c	2.2 ± 0.4^c
$WRPC_2$	10/90	2	893 ± 19^a	0.35 ± 0.03^a	2.11 ± 0.09^{ab}	46.7 ± 2.2^{bcd}	2.09 ± 0.04^{ab}	22.4 ± 1.6^c	2.2 ± 0.1^c
$WRPC_4$	10/90	4	883 ± 17^a	0.35 ± 0.03^a	2.25 ± 0.10^{ab}	46.4 ± 3.1^{bcd}	1.98 ± 0.03^{abc}	25.6 ± 1.3^b	2.7 ± 0.2^c
$WRPC_8$	10/90	8	897 ± 7^a	0.36 ± 0.01^a	2.25 ± 0.05^{ab}	47.6 ± 0.9^{abc}	2.00 ± 0.04^{abc}	24.9 ± 1.2^{bc}	2.6 ± 0.2^c
$WRPC_{13}$	10/90	13	910 ± 19^a	0.24 ± 0.01^b	2.33 ± 0.08^a	50.0 ± 1.3^{ab}	2.13 ± 0.06^a	26.0 ± 1.6^b	3.1 ± 0.3^{bc}
$WRPC_{23}$	10/90	23	885 ± 1^a	0.18 ± 0.01^c	1.82 ± 0.04^c	42.9 ± 0.4^d	1.82 ± 0.01^c	23.9 ± 0.3^{bc}	3.9 ± 0.2^b

Values are presented as the mean ± SD ($n = 5$). Different superscript letters within a column indicate significant differences among groups ($p < 0.05$).

particle/rPP interface. In addition, all of the WRPCs cause a dramatic decrease in the elongation at break compared with that of the neat rPP because rigid fillers were added into a plastic matrix. However, for the composites filled with acetylated wood particles, the elongation at break remarkably increased, especially for the $WRPC_{23}$. The explanation for this occurrence is that the rigidity of wood particles could be reduced by acetylation. A similar result was also reported by Pasquini et al. [30].

Observation of the fracture surfaces of the composites by SEM can provide insight into information related to interfacial adhesion [32]. The SEM micrographs of the tensile fractured surface for the composites samples are shown in Fig. 2. Although only selected portions of the WRPCs are shown in the figures, they are assumed to be as representative of the sample as possible. Accordingly, for the $WRPC_0$, the unmodified wood particles are pulled out nearly intact from the polymeric matrix (Fig. 2A), i.e., the fracture of the composite did not lead to breaking of the wood particles. This observation clearly indicates that the interfacial adhesion between the wood particle and the plastic was quite weak. A similar bonding characteristic was observed in $WRPC_2$ (Fig. 2B). However, as shown in Fig. 2C–F, the SEM micrographs reveal that acetylated wood particles are sufficiently trapped by the polymeric matrix, which provides evidence of good interfacial interaction if the WPG of acetylated wood particles is greater than 4%. Thus, better stress transfer from the weaker plastic phase to the wood particle through the interface could be expected. This effect is believed to be caused by improved interfacial interaction, which results in high flexural and tensile strength, as shown in Table 2.

3.2. Extended creep behavior of WRPCs assessed using the TTSP

This section outlines the use of the TTSP to predict the long-term creep behavior of composites from short-term accelerated creep tests at a range of elevated temperatures. The DMA method is appropriate for this test because it is capable of testing at a wide range of temperatures. Using $WRPC_0$ as an example, Fig. 3A shows the creep compliance with elevated temperature over the actual time for the entire duration, and Fig. 3B and C show the unshifted short-term creep compliance and corresponding master curves of $WRPC_0$ at all tested temperatures plotted against the test time on a log scale, respectively. For the shift factor, two methods can be used for WPCs: the William–Landel–Ferry (WLF) equation and the Arrhenius equation. For the WLF equation, the material is tested at working temperatures in the range from the glass-transition temperature (T_g) to T_g + 100 °C [33]. The rPP is appropriate for this method because the T_g of the thermoplastic is approximately 15 °C. Therefore, the WLF equation was used for WRPCs in this study. The shift factor can be related to temperature using the following equation:

$$\log \alpha_T = \frac{-C_1(T - T_{ref})}{(C_2 + T - T_{ref})} \tag{2}$$

$$C_1 = \frac{C_{1g}C_{2g}}{(C_{2g} + T_{ref} - T_g)} \tag{3}$$

$$C_2 = C_{2g} + T_{ref} - T_g \tag{4}$$

where α_T is the horizontal shift factor, T_{ref} is the reference temperature (K), T is the test temperature (K), and C_{1g} and C_{2g} are constants (17.44 and 51.6, respectively) [13,34–36].

According to the reduced time using a shift factor (α_T) calculated from the WLF equation, the creep curves at elevated temperatures were shifted to the right along the time axis. In addition, the long-term (experimental data) and TTSP-predicted creep compliance curves of $WRPC_0$ are shown in Fig. 3D. It revealed that the predicted creep compliance was slightly higher than that of the experimental results. This difference is mainly resulted from two events. One is the thermal expansion while heating the sample using the TTSP [37]; another is physical ageing which is presumed to be responsible for this discrepancy, because the long-term creep test during the application of the load leads to a stiffening of the material with increasing time [38]. However, the creep compliance was slightly overestimated by TTSP, but the predicted creep compliance curve showed consistent trend with the experimental data in the steady creep rate. This result demonstrated that the TTSP could be used to predict the long-term creep behavior of WRPCs.

Consequently, the creep compliance master curves of the various WRPCs generated using shift factors are estimated from the WLF equation. The master curves were modeled with the Findley power law [39], which is presented in following equation:

$$S(t) = S_0 + at^b \tag{5}$$

where $S(t)$ is the time-dependent compliance, S_0 is the instantaneous elastic compliance, a and b are constant numbers, and t is the elapsed

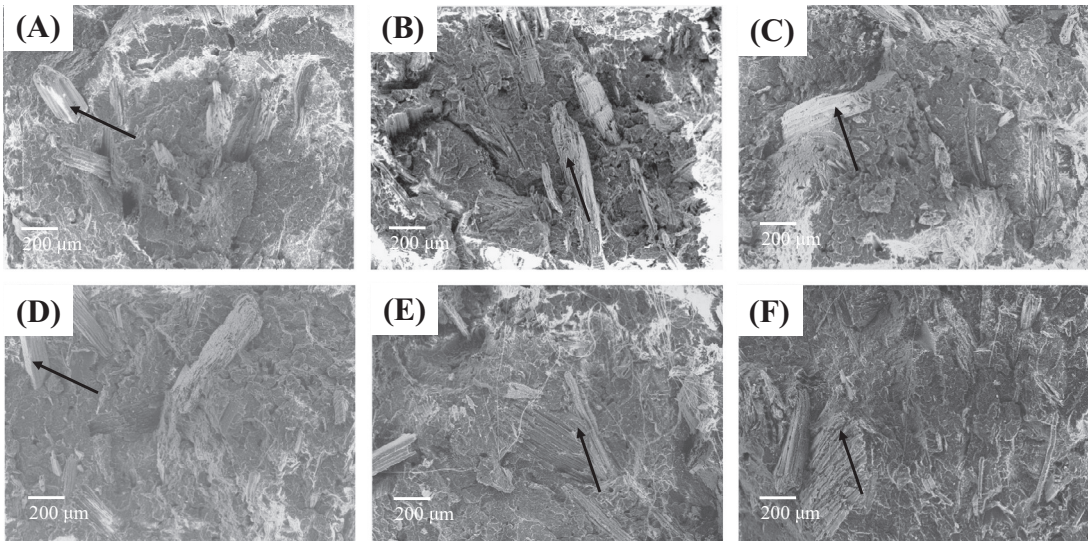

Fig. 2. Scanning electron microscopy (SEM) micrographs of WRPCs with different extents of acetylated wood particles. (A) $WRPC_0$; (B) $WRPC_2$; (C) $WRPC_4$; (D) $WRPC_8$; (E) $WRPC_{13}$; (F) $WRPC_{23}$. Arrows: Wood particle.

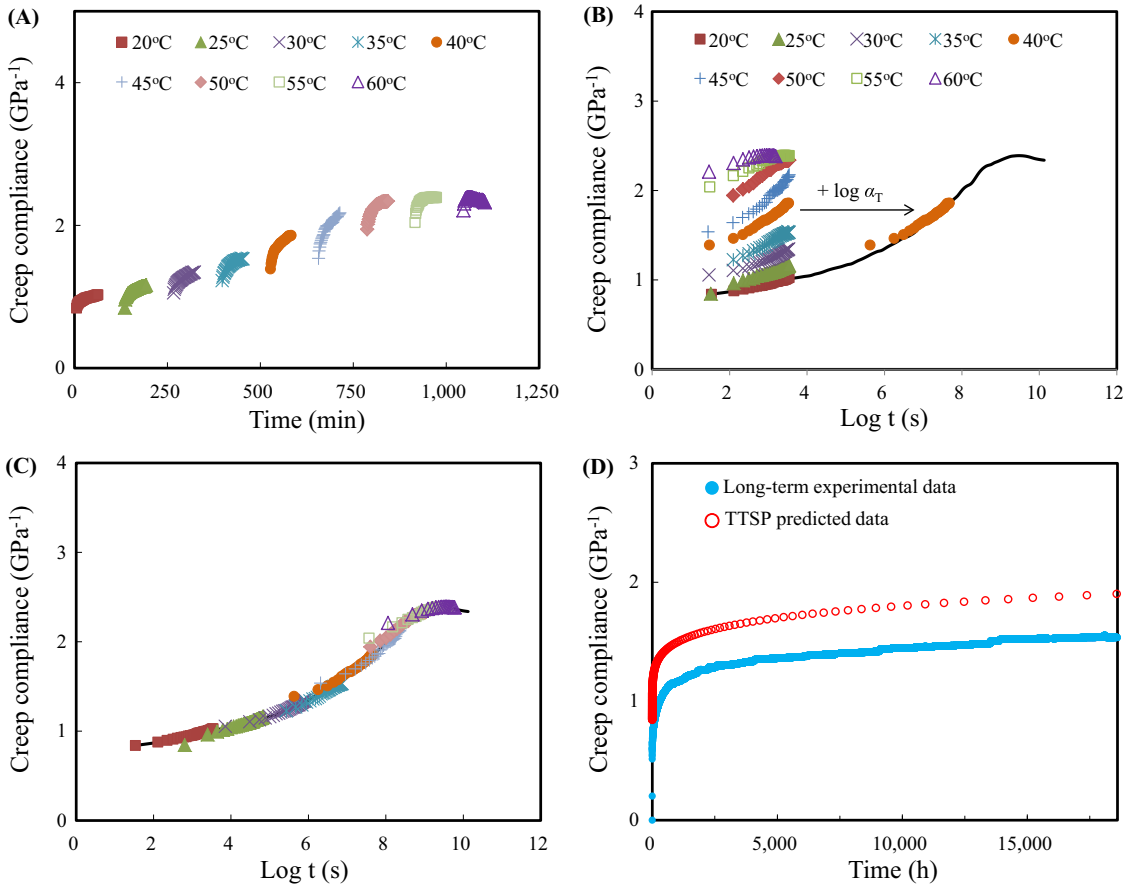

Fig. 3. (A) Creep compliance of $WRPC_0$ at elevated temperatures in the actual test. (B) Unshifted and shifted creep compliance and (C) corresponding master curve of unmodified WRPC using a reference temperature of 20 °C against the test time on a log scale. (D) Comparison of long-term creep compliance and TTSP predicted creep compliance for $WRPC_0$.

Table 3
Predicted creep compliances of various WRPCs using a reference temperature of 20 °C.

Specimen	S_0 (GPa^{-1})	a	b	R^2	$S(t)$ (GPa^{-1}) Time (years)					Improvement of creep resistance (%) Time (years)				
					1	5	10	20	30	1	5	10	20	30
$WRPC_0$	0.61	0.14	0.12	0.992	1.78	2.04	2.16	2.30	2.39	–	–	–	–	–
$WRPC_2$	0.60	0.06	0.14	0.994	1.33	1.53	1.62	1.73	1.80	25	25	25	25	25
$WRPC_4$	0.57	0.04	0.16	0.992	1.28	1.50	1.60	1.73	1.81	28	27	26	25	24
$WRPC_8$	0.54	0.06	0.13	0.993	1.19	1.35	1.43	1.51	1.57	33	34	34	34	35
$WRPC_{13}$	0.53	0.03	0.15	0.996	1.04	1.19	1.26	1.35	1.40	41	42	42	41	41
$WRPC_{23}$	0.55	0.04	0.18	0.993	1.39	1.68	1.83	2.01	2.12	22	17	15	13	11

$S(t) = S_0 + at^b$, where $S(t)$ is the time-dependent compliance, S_0 is the instantaneous elastic compliance, and a and b are constant values.

time. Accordingly, the Findley power law model fit the TTSP creep curves well for all WRPCs over the entire time period. As shown in Table 3, the R^2 values of all WRPCs are greater than 0.99. Furthermore, the creep curves of the various WRPCs on a log time scale are shown in Fig. 4A. The result revealed that the compliance of $WRPC_0$ was greater than that of WRPCs with acetylated wood particles and that the compliance decreased with increasing WPG up to 13%. In other words, among all WRPCs, the compliance of $WRPC_{13}$ was the lowest during the creep duration. When 23% WPG of acetylated wood particles were added in the rPP matrix, however, the compliance increased dramatically. Fig. 4B shows the creep master curves on a normal time scale, and the instantaneous elastic compliances (S_0) and the predicted the time-dependent compliances ($S(t)$) of all the WRPCs over 1–30 year periods are listed in Table 3. The S_0 of $WRPC_{13}$ was the lowest (0.53 GPa^{-1}) among all WRPCs. For the predicted compliance, $WRPC_0$ showed 1.78 GPa^{-1}, 2.04 GPa^{-1}, 2.16 GPa^{-1}, 2.30 GPa^{-1} and 2.39 GPa^{-1} at 1, 5, 10, 20 and 30 years, respectively. As expected, the compliance of WRPCs with acetylated wood particles declined dramatically. These results implied that the creep resistance of WRPCs could be enhanced through wood acetylation due to better interfacial interaction between the wood particle and the polymeric matrix. These findings are similar to the flexural and tensile properties data. Moreover, to estimate the creep resistance of a sample under long-term conditions, the improvement of creep resistance (*ICR*) was calculated using the following equation:

$$ICR\ (\%) = \left[1 - \frac{S(t)_a}{S(t)_u}\right] \times 100 \quad (6)$$

where $S(t)_a$ and $S(t)_u$ are the time-dependent compliance of acetylated and unmodified WRPCs, respectively. As shown in Table 3,

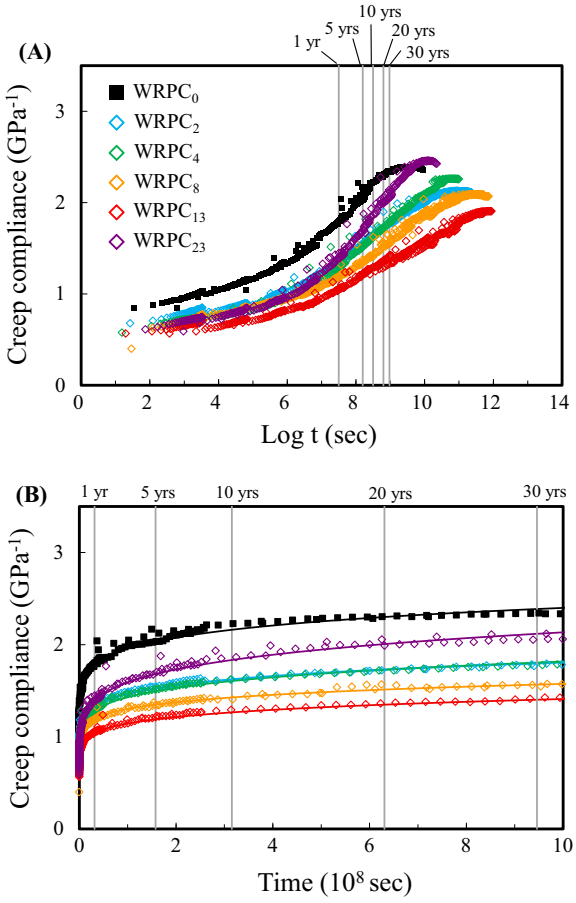

Fig. 4. Creep master curves of WRPCs with different extents of acetylated wood particles on a log time scale (A) and on a normal time scale (B) using a reference temperature of 20 °C.

the creep resistances of all acetylated WRPCs were improved in the range of 11–41% over a 30-year period. Of these data, the largest value was found for $WRPC_{13}$ (41%), and the smallest value was found for $WRPC_{23}$ (11%). Taken together, the results indicated that the $WRPC_{13}$ exhibited the best creep resistance.

4. Conclusions

Compared with unmodified wood particles, the acetylated wood particles exhibit excellent reinforcing effects on the mechanical properties and creep resistance of wood/recycled-polypropylene composites (WRPCs). The results revealed that the moisture content of WRPCs decreased with increasing the extent of wood acetylation, whereas the flexural and tensile properties of WRPCs were enhanced with increasing the WPG of acetylated wood particles up to 13%; however, these properties declined sharply as the WPG was further increased. In addition, among all WRPCs, the $WRPC_{13}$ exhibited the best creep resistance. The SEM micrographs revealed that acetylated wood particles are sufficiently trapped by the polymeric matrix. These results indicate that the interfacial interaction between the wood particle and the plastic plays a role in stress transition for improved mechanical and creep properties in a composite. Accordingly, the addition of acetylated wood particles in an rPP matrix can improve not only its tensile and flexural performances but also its creep resistance, especially with 13% WPG of acetylated wood particles. Therefore, these composites offer a high-performance alternative to conventional WPCs for building and construction applications.

Acknowledgement

This work was financially supported by a research grant from the Ministry of Science and Technology, Taiwan (MOST 104-2622-B-005-006-CC3).

References

[1] A.K. Bledzki, S. Reihmane, J. Gassan, Thermoplastics reinforced with wood fillers: a literature review, Polym. Plast. Technol. Eng. 37 (1998) 451–468.
[2] E. Tronc, C.A. Hernández-Escobar, R. Ibarra-Gómez, A. Estrada-Monje, J. Navarrete-Bolaños, E.A. Zaragoza-Contreras, Blue agave fiber esterification for the reinforcement of thermoplastic composites, Carbohydr. Polym. 67 (2007) 245–255.
[3] K.-C. Hung, J.-H. Wu, Mechanical and interfacial properties of plastic composite panels made from esterified bamboo particles, J. Wood Sci. 56 (2010) 216–221.
[4] R.M. Rowell, Chemical modification of wood, For. Prod. Abstr. 6 (1983) 363–382.
[5] G. Gardea-Hernández, R. Ibarra-Gómez, S.G. Flores-Gallardo, C.A. Hernández-Escobar, P. Pérez-Romo, E.A. Zaragoza-Contreras, Fast wood fiber esterification. I. Reaction with oxalic acid and cetyl alcohol, Carbohydr. Polym. 71 (2008) 1–8.
[6] C.-N. Yang, K.-C. Hung, T.-L. Wu, T.-C. Yang, Y.-L. Chen, J.-H. Wu, Comparisons and characteristics of slicewood acetylation with acetic anhydride by liquid phase, microwave, and vapor phase reactions, Bioresources 9 (2014) 6463–6475.
[7] Y. Ren, Y. Wang, L. Wang, T. Liu, Evaluation of intumescent fire retardants and synergistic agents for use in wood flour/recycled polypropylene composites, Constr. Build. Mater. 76 (2015) 273–278.
[8] M. Bengtsson, P. Gatenholm, K. Oksman, The effect of crosslinking on the properties of polyethylene/wood flour composites, Compos. Sci. Technol. 65 (2005) 1468–1479.
[9] S.K. Najafi, M. Tajvidi, E. Hamidinia, Effect of temperature, plastic type and virginity on the water uptake of sawdust/plastic composites, Eur. J. Wood Wood Prod. 65 (2007) 377–382.
[10] H.-C. Chen, T.-Y. Chen, C.-H. Hsu, Effects of wood particle size and mixing ratios of HDPE on the properties of the composites, Eur. J. Wood Wood Prod. 64 (2006) 172–177.
[11] K.B. Adhikary, S. Pang, M.P. Staiger, Dimensional stability and mechanical behaviour of wood–plastic composites based on recycled and virgin high-density polyethylene (HDPE), Compos. Part B-Eng. 39 (2008) 807–815.
[12] C.-H. Lee, T.-L. Wu, Y.-L. Chen, J.-H. Wu, Characteristics and discrimination of five types of wood–plastic composites by Fourier transform infrared spectroscopy combined with principal component analysis, Holzforschung 64 (2010) 699–704.
[13] A.J. Nuñez, N.E. Marcovich, M.I. Aranguren, Analysis of the creep behavior of polypropylene–wood flour composites, Polym. Eng. Sci. 44 (2004) 1594–1603.
[14] W.K. Goertzen, M.R. Kessler, Creep behavior of carbon fiber/epoxy matrix composites, Mat. Sci. Eng. A Struct. 421 (2006) 217–225.
[15] J. Chen, D.J. Gardner, Dynamic mechanical properties of extruded nylon-wood composites, Polym. Compos. 29 (2008) 372–379.
[16] P. Dasappa, P. Lee-Sullivan, X. Xiao, Temperature effects on creep behavior of continuous fiber GMT composites, Compos. Part A Appl. Sci. 40 (2009) 1071–1081.
[17] T.-C. Yang, T.-L. Wu, K.-C. Hung, Y.-L. Chen, J.-H. Wu, Mechanical properties and extended creep behavior of bamboo fiber reinforced recycled poly(lactic acid) composites using the time–temperature superposition principle, Constr. Build. Mater. 93 (2015) 558–563.
[18] N. Saba, M.T. Paridah, M. Jawaid, Mechanical properties of kenaf fibre reinforced polymer composite: a review, Constr. Build. Mater. 76 (2015) 87–96.
[19] S.-H. Lee, S. Wang, Biodegradable polymers/bamboo fiber biocomposite with bio-based coupling agent, Compos. Part A Appl. Sci. 37 (2006) 80–91.
[20] R. Tokoro, D.M. Vu, K. Okubo, T. Tanaka, T. Fujii, T. Fujiura, How to improve mechanical properties of polylactic acid with bamboo fibers, J. Mater. Sci. 43 (2008) 775–787.
[21] T.-L. Wu, Y.-C. Chien, T.-Y. Chen, J.-H. Wu, The influence of hot-press temperature and cooling rate on thermal and physicomechanical properties of bamboo particle-polylactic acid composites, Holzforschung 67 (2013) 325–331.
[22] C.-H. Lee, K.-C. Hung, Y.-L. Chen, T.-L. Wu, J.-H. Wu, Effects of polymeric matrix on accelerated UV weathering properties of wood–plastic composites, Holzforschung 66 (2012) 981–987.
[23] K.-C. Hung, Y.-L. Chen, J.-H. Wu, Natural weathering properties of acetylated bamboo plastic composites, Polym. Degrad. Stab. 97 (2012) 1680–1685.
[24] ASTM standard. D790–10, Standard test methods for flexural properties of unreinforced and reinforced plastics and electrical insulating materials, 2010.
[25] ASTM standard. D638–14, Standard test method for tensile properties of plastics, 2014.
[26] V. Tserki, N.E. Zafeiropoulos, F. Simon, C. Panayiotou, A study of the effect of acetylation and propionylation surface treatments on natural fibers, Compos. Part A Appl. Sci. 36 (2005) 1110–1118.
[27] S.K. Najafi, E. Hamidinia, M. Tajvidi, Mechanical properties of composites from sawdust and recycled plastics, J. Appl. Polym. Sci. 100 (2006) 3641–3645.

[28] S.-Y. Lee, S.-J. Chun, G.-H. Doh, I.-A. Kang, Influence of chemical modification and filler loading on fundamental properties of bamboo fibers reinforced polypropylene composites, J. Compos. Mater. 43 (15) (2009) 1639–1657.
[29] S. Ochi, Development of high strength biodegradable composites using Manila hemp fiber and starch-based biodegradable resin, Compos. Part A Appl. Sci. 37 (2006) 1879–1883.
[30] D. Pasquini, E.M. Teixeira, A.A.S. Curvelo, M.N. Belgacem, A. Dufresne, Surface esterification of cellulose fibres: processing and characterisation of low-density polyethylene/cellulose fibres composites, Compos. Sci. Technol. 68 (2008) 193–201.
[31] S. Thiebaud, M.E. Borredon, G. Baziard, F. Senocq, Properties of wood esterified by fatty-acid chlorides, Bioresour. Technol. 59 (1997) 103–107.
[32] H. Liu, Q. Wu, G. Han, F. Yao, Y. Kojima, S. Suzuki, Compatibilizing and toughening bamboo flour-filled HDPE composites: mechanical properties and morphologies, Compos. Part A Appl. Sci. 39 (2008) 1891–1900.
[33] J.D. Ferry, Viscoelastic Properties of Polymers, John Wiley & Sons, New York, 1980.
[34] M. Tajvidi, R.H. Falk, J.C. Hermanson, Time-temperature superposition principle applied to a kenaf fiber/high density polyethylene composites, J. Appl. Polym. Sci. 97 (2005) 1995–2004.
[35] Y. Xu, S.-Y. Lee, Q. Wu, Creep analysis of bamboo high-density polyethylene composites: effect of interfacial treatment and fiber loading level, Polym. Compos. 32 (2011) 692–699.
[36] Y. Xu, Q. Wu, Y. Lei, F. Yao, Creep behavior of bagasse fiber reinforced polymer composites, Bioresour. Technol. 101 (2010) 3280–3286.
[37] F. Achereiner, K. Engelsing, M. Bastian, P. Heidemeyer, Accelerated creep testing of polymers using the stepped isothermal method, Polym. Test. 32 (2013) 447–454.
[38] H.F. Brinson, L.C. Brinson, Polymer Engineering Science and Viscoelasticity, An Introduction, Springer, New York, 2008.
[39] W.N. Findley, J.S. Lai, K. Onaran, Creep and Relaxation of Nonlinear Viscoelastic Materials with an Introduction to Linear Viscoelasticity, Dover Publications, New York, 1976.